

## FEA OF IMPACT RESPONSES FOR DAMPED FRAME STRUCTURES SUPPORTED BY MULTIPLE NONLINEAR SPRINGS WITH HYSTERESIS

TAKAO YAMAGUCHI<sup>\*</sup>, CHEN YUAN<sup>\*</sup>, HISANORI TOMITA<sup>\*</sup>, MUHAMMAD  
TAUFIQ BIN IBRAHIM<sup>\*</sup>, SHINICHI MARUYAMA<sup>\*</sup>, MITSU HARU WATANABE<sup>†</sup>  
AND MANABU SASAJIMA<sup>†</sup>

<sup>\*</sup> Gunma University  
1-5-1 Tenjin-cho, Kiryu, 376-8515 Gunma, Japan  
e-mail: yamagume3@gunma-u.ac.jp, www.tech/gunma-u.ac.jp

<sup>†</sup> Foster Electric Co., Ltd.  
1-1-109, Tsutsujigaoka, Akishima, 196-8550 Tokyo, Japan

**Key Words:** *Simulation, Damping, Nonlinear Impact response, FEM.*

**Abstract.** This paper deals with nonlinear vibration analysis using finite element method for frame structures consisting of elastic and viscoelastic damping layers supported by multiple nonlinear concentrated springs with hysteresis damping. The frame is supported by four nonlinear concentrated springs near the four corners. The restoring forces of the springs have cubic non-linearity and linear component of the nonlinear springs has complex quantity to represent linear hysteresis damping. The damping layer of the frame structures has complex modulus of elasticity. Further, the discretized equations in physical coordinate are transformed into the nonlinear ordinary coupled differential equations using normal coordinate corresponding to linear natural modes. Comparing shares of strain energy of the elastic frame, the damping layer and the springs, we evaluate the influences of the damping couplings on the linear and nonlinear impact responses. We also investigate influences of damping changed by stiffness of the elastic frame on the nonlinear coupling in the damped impact responses.

### 1 INTRODUCTION

Springs are often used not only for heavy structures but also for lightweight structures such as parts in automobiles to insulate them from external vibrations and shocks. However, in many cases, the stiffness of a lightweight structure is not sufficiently high for the structure to be considered rigid. Thus, in dynamic analysis, it is necessary to deal with these structures as elastic bodies. If the structures comprise resins, they should be treated as viscoelastic bodies.

Many researchers have studied for the nonlinear vibrations of concentrated masses with springs [1]. The authors previously proposed a fast numerical method to compute the nonlinear vibrations in an elastic/viscoelastic block with a nonlinear spring [2].

To reduce vibrations, viscoelastic damping materials are often laminated on the metal structures. Damping characteristics (e.g. modal loss factors) of these laminated panels are

affected by not only properties of the viscoelastic materials but also stiffness of the metal panels. To calculate the modal loss factors, which corresponds to modal damping when the structure are deformed as eigenmodes at resonant frequencies, complex eigenvalue analysis are often used. To compute the modal loss factors using FEM under linear problem, Johnson proposed Modal Strain Energy Method (i.e. MSE Method) [3,4]. Using this method, the modal loss factors can be computed using material loss factor for each element and the ratio of modal strain energy for each element to total modal strain energy. This method is very useful to investigate damping mechanism in the metal structures with viscoelastic layers. However, there are few reports to treat nonlinear vibration problem of the metal structures with viscoelastic damping layers supported by nonlinear spring.

This paper describes vibration analysis using FEM for elastic structures with viscoelastic layers connected with nonlinear springs with hysteresis. We think this is a simplified model of a subframe supported by rubber mounts in automotive suspensions. The restoring force of the spring is expressed as power series of its deformation. A complex spring constant is introduced for the linear component of the restoring force. The finite elements for the nonlinear spring are expressed and they are attached to the elastic / viscoelastic structures, which are modeled as solid finite elements with a complex modulus of elasticity. We obtain the nonlinear discrete equations of motion for the whole structure. To get modal loss factors, we introduce small parameters concerning damping to complex eigenvalue problem of the equations under small deformation.

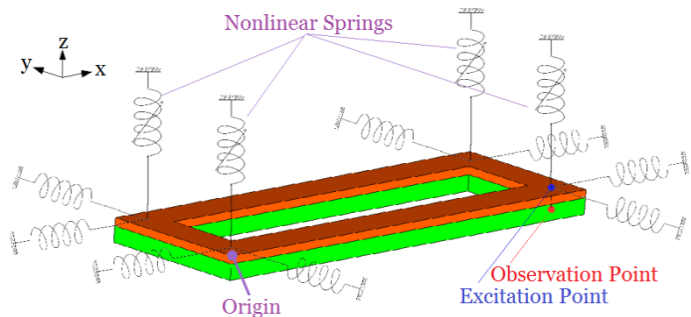


Figure 1: Simulation model

And we obtain asymptotic equations from the zero and first orders. Then, the approximate modal loss factors are obtained like MSE. Further, by introducing normal coordinate corresponding to eigenmodes, the nonlinear discrete equations in physical coordinates are transformed into nonlinear ordinary coupled equations. The transformed equations are rapidly computed to obtain the nonlinear transient responses with a fairly small dof.

As a numerical example of this proposed FEM, we deal with elastic frames with damping layers supported by multiple nonlinear springs with hysteresis. Using the proposed method, we show new phenomena including nonlinear coupling between nonlinear springs with hysteresis and elastic frames and viscoelastic layers. We clarify influences of amplitude of the impact force on nonlinear transient responses.

## 2 NUMERICAL MODEL

We use a simplified simulation model for frame structures supported by springs on four corners of the frame as shown in Figure 1. We set the origin at one corner as shown in Figure 1 in the  $x$   $y$  plane on the upper surface of the frame. There exist four nonlinear springs in the  $z$  direction on each four corners. Further, on these corners, linear springs are set both in the  $x$  and  $y$  directions. The frame structures are composed of a steel frame and a viscoelastic damping layer. Figure 2 shows three models which we investigate. The detail geometry of the

models are shown in this figure. “Elastic Frame Model” as shown in Figure 2 has only a steel frame. This has no viscoelastic damping layer. “Elastic Frame model with Damping Layer” has a steel frame with a damping layer. Thickness of the frame is 10mm and the thickness of the damping layer is 20mm. “High Stiffness Elastic Frame model with Damping Layer” has also a steel frame and a damping layer. But, thickness of the frame is 20mm which is twice of the thickness for “Elastic Frame model with Damping Layer”.

The concentrated nonlinear springs in the  $z$  direction have cubic nonlinearity in the relation between their displacement  $u_{mz}$  and their restoring force  $R_{mz}$  as shown in Figure 3. Linear hysteresis damping is introduced into the restoring force of the nonlinear springs. Namely, linear components of the spring constants have complex quantity as

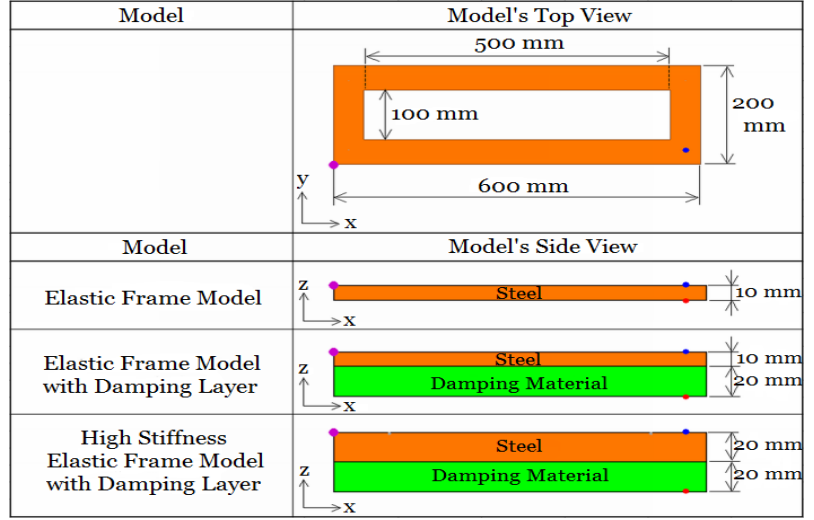
$\gamma_{1m} = \bar{\gamma}_{1mz}(1 + j\eta_s)$ .  $\eta_s$  shows the loss factor of the springs. Further, there also exist linear concentrated springs in  $x$  and  $y$  directions at the corners. These linear springs have the same complex quantity as the linear component of the nonlinear springs. As shown in Figure 1, the excitation point is  $(x, y, z) = (575, 30, 0)$  on the upper surface of the steel frame. We evaluate impact responses of this simulation model. The evaluation point is  $(x, y) = (575, 30)$  in Figure 2 on the bottom surface of the frame with the damping layer.

### 3 NUMERICAL METHOD

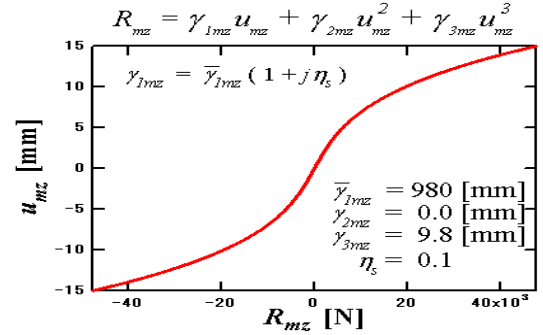
We demonstrate a numerical method to calculate nonlinear responses by considering coupled damping properties for the elastic structures having viscoelastic damping layers connected to the nonlinear concentrated springs with linear hysteresis damping.

#### 3.1 Discretized equation for the nonlinear concentrated springs with linear hysteresis

First, we show discretized equations for the nonlinear concentrated springs with linear hysteresis [2]. We assumed that the nonlinear concentrated springs with viscoelasticity have the principal elastic axes in the  $z$  direction as illustrated in Figure 1. We introduce the



**Figure 2:** Detail geometry of elastic frames with damping layer supported by nonlinear / linear springs



**Figure 3:** Restoring force of nonlinear springs

displacement as  $u_{mz}$ , ( $m=1,2,3,\dots$ ) in the  $z$  direction at the nodal points  $\alpha_m$ , ( $m=1,2,3,\dots$ ) where the nonlinear springs are attached with the steel frame. The nodal force at the point  $\alpha_m$  is expressed using the power series of  $u_{mz}$ . When cubic nonlinearity is assumed, the restoring force  $R_{mz}$  of the spring can be expressed as follows.

$$R_{mz} = \gamma_{1mz}u_{mz} + \gamma_{2mz}u_{mz}^2 + \gamma_{3mz}u_{mz}^3 \quad (1)$$

Next, linear hysteresis damping is introduced as  $\gamma_{1m} = \bar{\gamma}_{1mz}(1 + j\eta_s)$ .  $j$  is the imaginary unit.  $\bar{\gamma}_{1mz}$  is the real part of  $\gamma_{1m}$ , while  $\eta_s$  is the material loss factor of the spring. The relation in Equation (1) can be rewritten in the matrix form as follows:

$$\{R_m\} = [\bar{\gamma}_{1m}] \{u_m\} + \{\bar{d}_m\} \quad (2)$$

$$[\bar{\gamma}_{1m}] = \begin{bmatrix} 0 & 0 & 0 \\ 0 & 0 & 0 \\ 0 & 0 & \gamma_{1mz} \end{bmatrix}, \quad \{\bar{d}_m\} = \{0, 0, \gamma_{2mz}u_{mz}^2 + \gamma_{3mz}u_{mz}^3\} \quad (3)$$

where  $\{R_m\} = \{R_{mx}, R_{my}, R_{mz}\}^T$ ,  $R_{mx} = R_{my} = 0$  is the nodal force vector at the node  $\alpha_m$ .  $\{u_m\} = \{u_{mx}, u_{my}, u_{mz}\}^T$  is the nodal displacement vector at the node  $\alpha_m$ .  $[\bar{\gamma}_{1m}]$  is a complex stiffness matrix involving the linear term of the restoring force.  $\{\bar{d}_m\}$  is a vector containing the nonlinear terms of the restoring force.

### 3.2 Discretized equation for the elastic frame and the viscoelastic damping layer

For vibration of the steel frame and the viscoelastic damping material, we used discretized equations written in the following equations from Equations (4) and (5). They correspond to conventional linear finite element model in consideration of linear hysteresis damping.

$$[M_s]_e \{\ddot{u}_s\}_e + [K_s]_e \{u_s\}_e = \{f_s\}_e \quad (4)$$

$[K_s]_e$  and  $[M_s]_e$  are the element stiffness matrix and element mass matrix, respectively.  $\{f_s\}_e$  and  $\{u_s\}_e$  are the nodal force vector and nodal displacement vector in an element  $e$ .

By replacing complex modulus of elasticity with real modulus of elasticity, the viscoelastic damping layer can be modeled using finite elements. Consequently, the element stiffness matrix  $[K_s]_e$  in Equation (4) becomes to have complex quantities in Equation (5).

$$[K_s]_e = [K_{sR}]_e (1 + j\eta_{se}) \quad (5)$$

$[K_{sR}]_e$  is the real part of element stiffness matrix for the viscoelastic material.  $\eta_{se}$  is the material loss factor corresponding to each element  $e$ .

For the elastic and the viscoelastic materials, isoparametric hexahedral elements with the non-conforming modes [5] are chosen. For the viscoelastic damping material, the storage modulus of elasticity is  $8.00 \times 10^8$  [N/m<sup>2</sup>], the mass density is  $1.45 \times 10^3$  [kg/m<sup>3</sup>] and the material loss factor  $\eta_{se}$  is 0.333.

### 3.3 Discrete equations for the global system between the linear / nonlinear springs and the elastic frame with the viscoelastic damping layer

The restoring force  $\{R_m\}$  in Equation (2) is added to the nodal force at the connected nodes  $\alpha_m$  between the nonlinear concentrated springs in the  $z$  direction and the elastic frame. Further, the linear springs in the  $x$  and  $y$  directions are also attached. The next equation can be obtained for the global system [2]:

$$[M]\{\ddot{u}\} + [K]\{u\} + \{\hat{d}\} = \{f\}, \{\hat{d}\} = \sum_m \{\hat{d}_m\} \quad (6)$$

where  $\{f\}$ ,  $[K]$ ,  $[M]$ , and  $\{u\}$  are the external force vector, complex stiffness matrix, mass matrix, and displacement vector in the global system, respectively.  $\{\hat{d}_m\}$  is modified from  $\{\bar{d}_m\}$  to have a vector size identical to dof of the global system.

### 3.4 Computation of modal loss factors

Next, we explain a computation method to obtain modal damping (i.e. modal loss factor) for the concentrated springs and the solid bodies (i.e. the elastic frame with the viscoelastic damping layer) in the global system. We neglect the nonlinear term under small deformation and the external force because of resonance conditions in Equation (6). Next, it is assumed that  $\{u\}$  can be expressed as  $\{u\} = \{\phi\}e^{j\omega t}$ .  $\omega$  and  $t$  represent the angular frequency and the time, respectively. Consequently, we have homogeneous equation of Equation (6), which corresponds to complex eigenvalue problem.

$$\sum_{e=1}^{e_{\max}} ([K_R]_e (1 + j\eta_e) - (\omega^{(i)})^2 (1 + j\eta_{tot}^{(i)}) [M]_e) \{\phi^{(i)}\} = \{0\} \quad (7)$$

In this equation,  $\eta_e$  is the elements' material loss factors which includes  $\eta_s$  and  $\eta_{se}$ .  $(\omega^{(i)})^2$  is the real part of complex eigenvalue. Superscript  $(i)$  stands for the  $i$ -th eigenmode.  $\{\phi^{(i)}\}$  is the complex eigenvector.  $\eta_{tot}^{(i)}$  is the modal loss factor. Next, we introduce the following  $\beta_{se}$  using the maximum value  $\eta_{\max}$  among the elements' material loss factors  $\eta_e$ , ( $e=1,2,3,\dots,e_{\max}$ ).

$$\beta_{se} = \eta_e / \eta_{\max}, \beta_{se} \leq 1 \quad (8)$$

If we assume  $|\eta_{\max}| \ll 1$ , solutions (i.e. complex eigenvalues and complex eigenvectors) of Equation (7) are expanded [4,7] using a small parameter  $\mu = j\eta_{\max}$ :

$$\{\phi^{(i)}\} = \{\phi^{(i)}\}_0 + \mu\{\phi^{(i)}\}_1 + \mu^2\{\phi^{(i)}\}_2 + \dots \quad (9)$$

$$(\omega^{(i)})^2 = (\omega_0^{(i)})^2 + \mu^2(\omega_2^{(i)})^2 + \mu^4(\omega_4^{(i)})^2 + \dots \quad (10)$$

$$j\eta_{tot}^{(i)} = \mu\eta_1^{(i)} + \mu^3\eta_3^{(i)} + \mu^5\eta_5^{(i)} + \mu^7\eta_7^{(i)} + \dots \quad (11)$$

Under conditions of  $\beta_{se} \leq 1$  and  $|\eta_{\max}| \ll 1$ , we can obtain  $|\eta_{\max}\beta_{se}| \ll 1$ . Thus,  $\mu\beta_{se}$  can be regarded as small parameters like  $\mu$ . In Equations (9),(10) and (11),  $\{\phi^{(i)}\}_0, \{\phi^{(i)}\}_1, \{\phi^{(i)}\}_2$

,... and  $(\omega_0^{(i)})^2, (\omega_2^{(i)})^2, (\omega_4^{(i)})^2, \dots$  and  $\eta_1^{(i)}, \eta_3^{(i)}, \eta_5^{(i)}, \dots$  have real quantities. By substitution of these equations from Equations (9) to (11) into Equation (7), we obtain approximate equations using  $\mu^0$  and  $\mu^1$  orders. Finally, the following equation can be derived by arranging the approximate equations:

$$\eta_{tot}^{(i)} = \sum_{e=1}^{e_{\max}} (\eta_e S_{se}^{(i)}) \quad (12)$$

From Equation (12), modal loss factor  $\eta_{tot}^{(i)}$  can be calculated using material loss factors  $\eta_e$  of each element  $e$  and share  $S_{se}^{(i)}$  of strain energy of each element to total strain energy. Equation (12) has the same form of MSE Method [3, 4] proposed by Johnson. This method helps us to decrease computational time for large-scale finite element models for the damped structure. And in Equation (12),  $\eta_e S_{se}^{(i)}$  corresponds to contribution of each element  $e$  to  $i$ -the modal damping. Using this, we can analyze coupled damping properties in the elastic frame with viscoelastic damping layer supported by complex springs having linear hysteresis.

### 3.5 Conversion to nonlinear equations in normal coordinates from equations in physical coordinate

When we compute impact responses using Equation (6) in physical coordinates directly, it takes considerable computational time. We adopt a numerical procedure to diminish the degree of freedom for the discretized equations of motion [2, 6].

We assume that the linear natural modes of vibration  $\{\phi^{(i)}\}$  can be approximated to  $\{\phi^{(i)}\}_0$ . Further, the nodal displacement vector can be expressed by introducing normal coordinates  $\tilde{b}_i$  corresponding to the linear natural modes  $\{\phi^{(i)}\}_0$  as follows:

$$\{u\} = \sum_i \tilde{b}_i \{\tilde{\phi}^{(i)}\}_0 / n_i \quad (13)$$

$$m_i = \{\phi^{(i)}\}_0^T [M] \{\phi^{(i)}\}_0, \{\tilde{\phi}^{(i)}\}_0^T [M] \{\tilde{\phi}^{(i)}\}_0 = 1, \{\phi^{(i)}\}_0 = \sqrt{m_i} \{\tilde{\phi}^{(i)}\}_0 = \{\tilde{\phi}^{(i)}\}_0 / n_i, n_i = 1 / \sqrt{m_i}.$$

By substitution of Equation (13) into Equation (6), the following nonlinear ordinary simultaneous equations with regard to normal coordinates  $\tilde{b}_i$  can be obtained.

$$\begin{aligned} \ddot{\tilde{b}}_i + \eta_{tot}^{(i)} \omega^{(i)} \dot{\tilde{b}}_i + (\omega^{(i)})^2 \tilde{b}_i + \sum_j \sum_k \tilde{D}_{ijk} \tilde{b}_j \tilde{b}_k + \sum_j \sum_k \sum_l \tilde{E}_{ijkl} \tilde{b}_j \tilde{b}_k \tilde{b}_l - \tilde{P}_i &= 0 \\ \tilde{P}_i = n_i \{\tilde{\phi}^{(i)}\}_0^T \{f\}, \{\tilde{\phi}^{(i)}\}_0 &= \{\tilde{\phi}_{i1x}, \tilde{\phi}_{i1y}, \tilde{\phi}_{i1z}, \tilde{\phi}_{i2x}, \tilde{\phi}_{i2y}, \tilde{\phi}_{i2z}, \tilde{\phi}_{i3x}, \dots\}^T \\ \tilde{D}_{ijk} = \sum_{m=1}^4 \tilde{\gamma}_{2mz} (n_i / (n_j n_k)) \tilde{\phi}_{imz} \tilde{\phi}_{jmz} \tilde{\phi}_{kmz}, \tilde{E}_{ijkl} &= \sum_{m=1}^4 \tilde{\gamma}_{3mz} (n_i / (n_j n_k n_l)) \tilde{\phi}_{imz} \tilde{\phi}_{jmz} \tilde{\phi}_{kmz} \tilde{\phi}_{lmz} \end{aligned} \quad (14)$$

We can save considerable computational time because Equation (14) has a much smaller degree of freedom than Equation (6).  $\tilde{\phi}_{imz}$  is the  $z$ -component of the eigenmode  $\{\tilde{\phi}^{(i)}\}_0$  at the  $m$ -th connected node  $\alpha_m$  between the frame and the nonlinear springs. The damping term in

Equation (14) can be derived in an identical form to Equation (12).

## 4 NUMERICAL RESULTS AND DISCUSSION

### 4.1 Results of modal loss factors, resonant frequencies and eigenmodes


















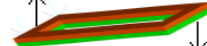




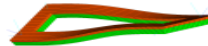
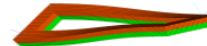














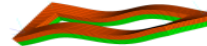



Tables 1 and 2 show eigenmodes  $\{\tilde{\phi}^{(i)}\}_0$ , resonant frequencies  $\omega_0^{(i)}/(2\pi)$  and modal loss factors  $\eta_{tot}^{(i)}$  for modes 1 to 14 and modes 15 to 21, respectively.

In these tables, arrows stand for directions of rigid motions in eigenmodes especially.

We give the material loss factors of the steel frames as  $\eta_e = \eta_f = 0.001$ . And that of the viscoelastic damping layer is  $\eta_e = \eta_d = 0.333$ . That of the springs is  $\eta_e = \eta_s = 0.100$ .

In these tables, results for the three models are shown. Results of ‘‘Elastic Frame Model’’ in Figure 2 are the left deformation pattern in Tables 1 and 2. Results of ‘‘Elastic Frame

**Table 1:** Vibration modes for mode 1 to mode 14

Vibration Mode	Elastic	Elastic with Damping Layer	High Stiffness Elastic with Damping Layer
1			
Frequency [Hz]	70.309	65.346	78.086
Modal Loss Factor	0.0214	0.0722	0.0964
2			
Frequency [Hz]	103.096	90.813	79.086
Modal Loss Factor	0.0564 *	0.082 *	0.0813 *
3			
Frequency [Hz]	134.924	116.144	88.397
Modal Loss Factor	0.0971 *	0.0966 *	0.0998
4			
Frequency [Hz]	135.910	116.499	93.775
Modal Loss Factor	0.0996	0.0997	0.0963
5			
Frequency [Hz]	181.822	158.350	122.898
Modal Loss Factor	0.0828 *	0.0945 *	0.0994
6			
Frequency [Hz]	188.555	161.159	126.647
Modal Loss Factor	0.099 *	0.0988 *	0.0985
7			
Frequency [Hz]	241.390	211.710	264.202
Modal Loss Factor	0.0777	0.0901	0.0351
8			
Frequency [Hz]	242.662	217.319	330.034
Modal Loss Factor	0.0412	0.0672	0.0220
9			
Frequency [Hz]	303.581	272.036	442.649
Modal Loss Factor	0.0424	0.0715	0.0198
10			
Frequency [Hz]	391.082	362.817	601.750
Modal Loss Factor	0.0172	0.0658	0.0031
11			
Frequency [Hz]	593.296	537.759	681.278
Modal Loss Factor	0.0116	0.0175	0.0172
12			
Frequency [Hz]	655.446	543.185	739.468
Modal Loss Factor	0.0010	0.0560	0.0042
13			
Frequency [Hz]	700.504	650.177	1016.703
Modal Loss Factor	0.0014	0.0467	0.0151
14			
Frequency [Hz]	807.193	694.289	1048.078
Modal Loss Factor	0.0031	0.0072	0.0053

Model with Damping Layer” in Figure 2 are the central deformation pattern in the tables. Results of “High Stiffness Elastic Frame Model with Damping Layer” in Figure 2 are the right deformation pattern in the tables.

**(1) Results of “Elastic Frame Model”**

In this paper, material loss factor  $\eta_s = 0.100$  of the springs are larger than  $\eta_f = 0.001$  of the steel frame. If eigenmodes include no elastic deformation of the steel frame, the modal loss factors are close to  $\eta_s = 0.100$ . Thus, modal loss factor  $\eta_{tot} = 0.996$  of mode 4 (i.e. rigid mode of the frame) is larger than  $\eta_{tot} = 0.0014$  for mode 13 (i.e. elastic mode of the steel frame).

Because the deformation of the springs is dominant in mode 4, the share of the strain energy in Equation (12) in the springs is large. This leads to high modal loss factor. On the other hand, the deformation of the springs are small in modes from 10 to 20 due to the elastic mode of the steel frame without damping layer. This leads to low modal loss factor.

For mode 2 including both rotation of the steel frame about the  $x$  axis and elastic deformation of the frame, the modal loss factor  $\eta_{tot} = 0.0564$  is middle value between those for mode 4 and mode 13. These phenomena are generated due to dependence of eigenmodes on the share of the strain energy in Equation (12).

**(2) Results of “Elastic Frame Model with Damping Layer”**

Modal loss factor  $\eta_{tot}$  of mode 10 for “Elastic Frame Model with Damping Layer” is larger than that of mode 10 for “Elastic frame Model”. Because the viscoelastic damping material has high material loss factor  $\eta_d = 0.333$ , modal loss factors  $\eta_{tot}$  for modes from 10 to 20 including elastic deformation of the frame increase.

**Table 2:** Vibration modes for mode 15 to mode 21

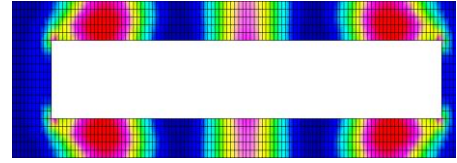
Vibration Mode	Elastic	Elastic with Damping Layer	High Stiffness Elastic with Damping Layer
15			
Frequency [Hz]	825.121	735.879	1196.660
Modal Loss Factor	0.0026	0.0511	0.0159
16			
Frequency [Hz]	956.608	836.983	1384.911
Modal Loss Factor	0.0023	0.0422	0.0166
17			
Frequency [Hz]	1126.364	928.771	1569.649
Modal Loss Factor	0.0024	0.0391	0.0153
18			
Frequency [Hz]	1148.874	1031.193	1633.472
Modal Loss Factor	0.0011	0.0531	0.0095
19			
Frequency [Hz]	1148.976	1038.075	1811.926
Modal Loss Factor	0.0028	0.0192	0.0160
20			
Frequency [Hz]	1375.819	1208.082	2009.518
Modal Loss Factor	0.0019	0.0548	0.0164



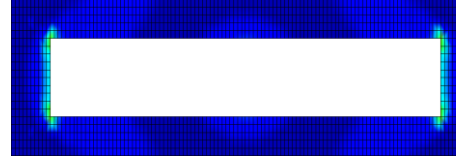
If we assume to remove the springs, we set that modal loss factors  $\eta_{tot}$  of the laminate (i.e. 10mm thickness of the steel frame plus 10mm thickness of the damping layer) are less than the material loss factor  $\eta_s=0.100$  of the springs. Therefore,  $\eta_{tot}=0.997$  of mode 4 including larger deformations in the springs is larger than  $\eta_{tot}=0.0467$  of mode 13 including larger elastic deformation in the steel frame. Modal loss factor  $\eta_{tot}=0.0564$  of mode 2 shows a middle value between them (i.e. modes 4 and 13) because this mode contains both elastic deformation in the steel frame and the deformation in springs when rotating motions of the frame occur.

### (3) Results of “High Stiffness Elastic Frame Model with Damping Layer”

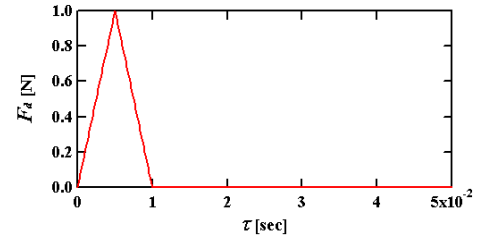
Because thickness of the steel frame for this model is 20mm, which is double for “Elastic Frame Model with Damping Layer”, this frame has higher stiffness. However, due to this high rigidity, damping decrease for modes from 10 to 20 having large deformation in the frame. For instance, modal loss factor  $\eta_{tot}=0.0166$  of this model for mode 16 is less than  $\eta_{tot}=0.0511$  of “Elastic Frame Model with Damping Layer” for mode 15. According to Equation (12), not only material loss factors but also share of strain energy are required to increase modal loss factors. Therefore, to increase modal loss factors of the frame with the damping layer, high share of the strain energy in the viscoelastic damping layer is required. Actually, we can find lower share of strain energy of the steel frame for “Elastic Frame Model with Damping Layer” as shown in Figure 5 than that for “High Stiffness Elastic Frame Model with Damping Layer” as shown in Figure 4. Using the proposed method, This phenomenon can be also explained roughly by Oberst expression [8] from theoretical analysis using complex flexural rigidity for bending vibrations of a beam having a non-constraint type viscoelastic damping layer. Damping becomes low when neutral plane of the frame with viscoelastic layer is apart from the



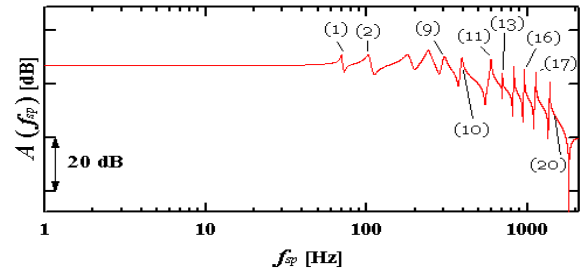
**Figure 4:** Strain energy distribution in steel frame for “High Stiffness Elastic Frame Model with Damping Layer” (Mode 16)



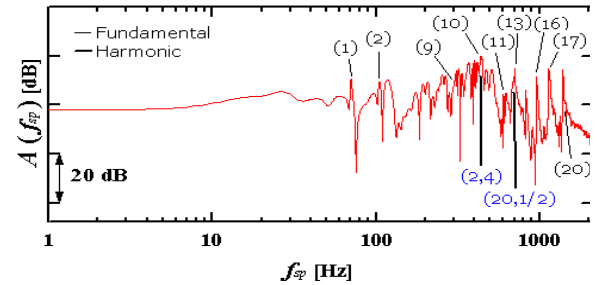
**Figure 5:** Strain energy distribution in steel frame for “Elastic Frame Model with Damping Layer” (Mode 15)



**Figure 6:** Time history of impact force



**Figure 7:** Fourier spectrum of impact response for “Elastic Frame Model” under small input ( $|F_{max}| = 0.98 \text{ N}$ )



**Figure 8:** Fourier spectrum of impact response for “Elastic Frame Model” under large input ( $|F_{max}| = 9.8 \times 10^5 \text{ N}$ )

damping layer.

As we mentioned before, this model has the thick frame. Due to high stiffness of the frame, elastic deformations of the steel frame become very small in modes 1 to 6, which we can almost regard as rigid motions for the frame. This leads that modal loss factors for these modes are close to the value of the material loss factor  $\eta_s=0.100$  of the springs.

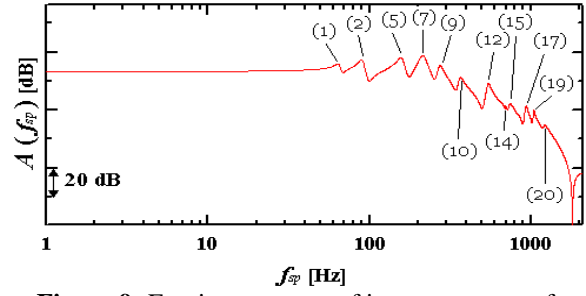
## 4.2 Results of impact responses

By changing the maximum amplitude  $|f_{\max}|$  of the impact as shown in Figure 6 under a constant pulse width 0.001 [s], transient time histories are computed. In Figure 6, the ordinate  $F_d$  represents force amplitude, while the abscissa  $\tau$  shows time. And we evaluate displacement at the evaluation point on the frame as shown in Figure 1.

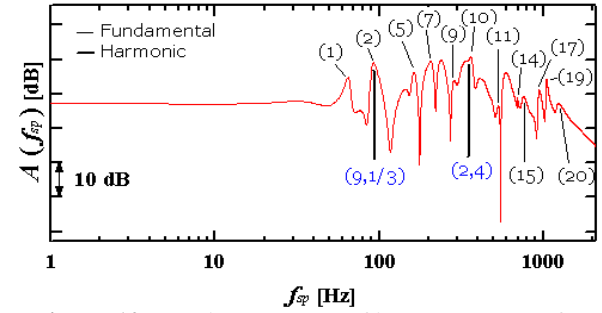
### (1) Results of “Elastic Frame Model”

Figure 7 represents the frequency response function of a time history under the small impact force  $|f_{\max}|=0.98[\text{N}]$ . And Figure 8 shows the frequency response function of the time history under the extraordinary large impact force  $|f_{\max}|=9.8\times 10^5[\text{N}]$ . In Figures 7 and 8, the ordinate represents amplitude of frequency response function  $A(f_{sp})$ , while the abscissa shows Fourier frequency  $f_{sp}$ . As for  $(m)$  in Figure 7,  $m$  denotes  $m$ -th vibration mode. For  $(m, n)$  in Figure 8,  $m$  denotes  $m$ -th vibration mode and  $n$  denotes types of the frequency response function. For instance,  $n=3$  shows super-harmonic component of the third order and  $n=1/2$  represents sub-harmonic component of the 1/2 order. 0 [dB] represents the amplitude of the spectrum equals 1[mm] for  $A(f_{sp})$  in these figures.

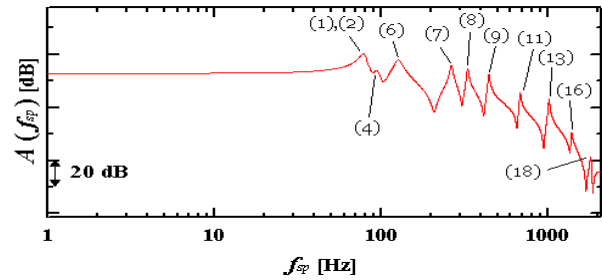
Under the small input force  $|f_{\max}|=0.98$  [N] in Figure 7, the peaks of the modes 1,2,5,7,9, 10,11,13,15,16,17 and 20 appear in the



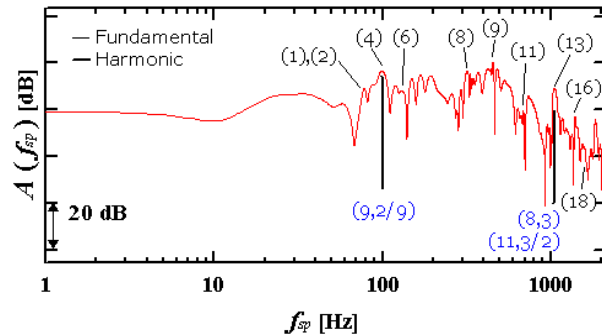
**Figure 9:** Fourier spectrum of impact response for “Elastic Frame Model with Damping Layer” under small input ( $|F_{\max}|=0.98$  N)



**Figure 10:** Fourier spectrum of impact response for “Elastic Frame Model with Damping Layer” under large input ( $|F_{\max}|=9.8\times 10^5$  N)



**Figure 11:** Fourier spectrum of impact response for “High Stiffness Elastic Frame Model with Damping Layer” under small input ( $|F_{\max}|=0.98$  N)



**Figure 12:** Fourier spectrum of impact response for “High Stiffness Elastic Frame Model with Damping Layer” under large input ( $|F_{\max}|=9.8\times 10^5$  N)

frequency response function mainly. Because excitation force in the  $z$  direction is acted on and the direction of observation is  $z$ , these modes include large amplitudes in the  $z$  direction.

Due to small modal loss factors including large elastic deformations in the steel frame and small deformation in the springs with linear hysteresis, the peaks for modes from 10 to 20 show sharp and have large amplitudes.

Under the extraordinary large input force  $|f_{\max}|=9.8\times 10^5$  [N] in Figure 8, there exist many peaks (i.e. not only fundamental components but also super harmonic, subharmonic components and internal resonances) for modes including large deformation in the nonlinear springs in the frequency response function.

### **(2) Results of “Elastic Frame Model with Damping Layer”**

We investigate of linear and nonlinear transient responses for “Elastic Frame Model with Damping Layer”. Figure 9 represents the frequency response function of a time history under the small impact force  $|f_{\max}|=0.98$  [N]. Figure 10 shows the frequency response function under the extraordinary large impact force  $|f_{\max}|=9.8\times 10^5$  [N].

Under the small input force  $|f_{\max}|=0.98$  [N] in Figure 9, the peaks of the modes 1,2,5,7,9, 10,11,13,15,16,17 and 20 appear in the frequency response function like Figure 7 for the model without damping layer. However, the amplitudes decrease for the peaks for modes from 10 to 20 including large deformations in the frame with damping layer. On the other hand, in comparison with Figure 7, there exist small changes in the peaks for modes 3,4 and 6 including large deformation in the springs and small deformations in the frame.

Under the extraordinary large input force  $|f_{\max}|=9.8\times 10^5$  [N] in Figure 10, in comparison with Figure 8 for the model without damping layer, number of the nonlinear peaks decrease. Especially, due to higher damping, this phenomenon is outstanding for modes from 10 to 20 including large deformation in the frame with the damping layer. Therefore, the damping layer enable us to diminish the nonlinear coupling in the transient response.

### **(3) Results of “High Stiffness Elastic Frame Model with Damping Layer”**

Next, we investigate of the transient responses for “High Stiffness Elastic Frame Model with Damping Layer” and clarify influences of the stiffness of the steel frame on linear / nonlinear transient responses. As we stated previously in Section 4.1, modal loss factors of this model decrease due to high stiffness of the steel frame for modes 10 to 20 containing large deformations in the frame with the damping layer. Figure 11 represents the frequency response function of a time history under the small impact force  $|f_{\max}|=0.98$  [N]. Figure 12 shows the frequency response function of a time history under the extraordinary large impact force  $|f_{\max}|=9.8\times 10^5$  [N].

Under the small input force  $|f_{\max}|=0.98$  [N] in Figure 11, the peaks of the modes 1,2,4,6,7, 9,11,13,16 and 18 appear in the frequency response function like Figures 9 for “Elastic Frame Model with Damping Layer”. Nevertheless, the amplitudes increase for the peaks for modes from 10 to 20 including large deformations in the frame with damping layer. This phenomenon is caused by low modal loss factors of these modes due to high stiffness of the steel frame as we explained in section 4.1.

Under the extraordinary large input force  $|f_{\max}|=9.8\times 10^5$  [N] in Figure 12, in comparison with Figure 10 for the model without damping layer, number of the nonlinear peaks increase.

Especially, due to lower damping oriented from high stiffness of the steel frame, this phenomenon is notable for modes from 10 to 20 including large deformation in the frame with the damping layer. Therefore, if we increase the thickness of the steel frame, damping of the frame with the damping layer diminishes and this leads to magnify the nonlinear coupling in the transient response, concequently.

## 5 CONCLUSIONS

This paper describes vibration analysis using FEM for elastic frames with viscoelastic layers connected with multiple nonlinear springs with hysteresis. The restoring force of the spring is expressed as power series of its elongation. A complex spring constant is introduced for the linear component of the restoring force. The finite elements for the nonlinear spring are expressed and they are attached to the elastic / viscoelastic structures, which are modeled as solid finite elements with a complex modulus of elasticity. To get modal loss factors, we introduce small parameters concerning damping to complex eigenvalue problem of the equations under small deformation. And we obtain asymptotic equations from the zero and first orders. Then, the approximate modal loss factors are obtained like MSE. Further, by introducing normal coordinate corresponding to eigenmodes. the nonlinear discrete equations in physical coordinates are transformed into nonlinear ordinary coupled equations.

We show phenomena including nonlinear coupled damped motions between nonlinear springs with hysteresis and elastic frames and viscoelastic layers by increasing impact force. Under a very large impact force as a severe condition, there exist complicated nonlinear couplings in Fourier spectrum. Due to high damping oriented from viscoelastic damping layer, nonlinear peaks are diminished. When we increase thickness of the steel frame, damping of the frame with the viscoelastic layer decrease. This causes the spectrum of the transient response includes more peaks due to nonlinear couplings.

## REFERENCES

- [1] E. Pesheck, N. Boivin, C. Pierre and S. W. Shaw, Non-linear modal analysis of structural systems using multi-mode invariant manifolds, *Nonlinear Dynamics* (2001) **25** :183-205.
- [2] T. Yamaguchi, Y. Fujii, K. Nagai and S. Maruyama, FEM for vibrated structures with nonlinear concentrated spring having hysteresis, *Mechanical Systems and Signal Processing* (2006) **20**: 1905-1922.
- [3] C. D. Johnson and D. A. Kienholz, Finite element prediction of damping structures with constrained viscoelastic layers, *AIAA Journal* (1982) **20** (9) :1284-1290.
- [4] B. A. Ma and J. F. He, A finite element analysis of viscoelastically damped sandwich plates, *Journal of Sound and Vibration* (1992) **152** (1) 107-123.
- [5] Zienkiewicz, O.C. and Taylor, R.L. *The finite element method*. McGraw Hill, Vol. I., (1989), Vol. II, (1991).
- [6] Yamaguchi, T. and Nagai, K., Chaotic vibration of a cylindrical shell-panel with an in-plane elastic support at boundary, *Nonlinear Dynamics* (1997) **13**:259-277.
- [7] Yamaguchi, T., Kurosawa, Y. and Enomoto, H., Damped vibration analysis using finite element method with approximated modal damping for automotive double walls with a porous material, *Journal of Sound and Vibration* (2009) **325**:436-450.
- [8] Oberst, H., *Akustische Beihefte* (1952) **4** :181-194.